Available online at www.sciencedirect.com

ScienceDirect

Mendeleev Commun., 2023, **33**, 657–660

Mendeleev Communications

Quantum chemical study of the activator contribution to stereoinduction at the step of alkene insertion into the catalytically active centers $Cp_2ZrMe(Cl)$–methylalumoxane

Denis N. Islamov, Tatyana V. Tyumkina* and Lyudmila V. Parfenova

Institute of Petrochemistry and Catalysis, Ufa Federal Research Centre of the Russian Academy of Sciences, 450075 Ufa, Russian Federation. E-mail:ttvnmr@gmail.com

DOI: 10.1016/j.mencom.2023.09.022

Quantum chemical modeling of the mechanism of asymmetric induction in the course of alkene (propene, hex-1-ene) coordination with $Cp_2ZrMe(Cl)$–methylalumoxane stereoisomeric complexes, which could act as catalytically active centers of the alkene oligomerization and polymerization, was carried out. A significant influence of the relative configuration of the chiral centers at the Al atoms of the activator on the parameters of the alkene insertion into Zr–C bond of the complexes was shown.

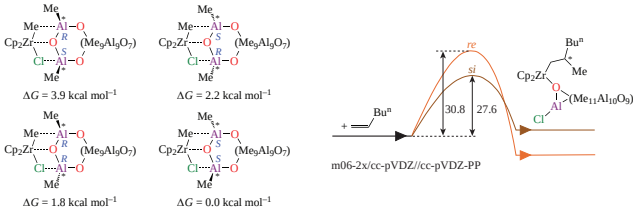

Keywords: Ziegler–Natta catalysis, methylalumoxane, alkene oligomerization, stereoselectivity, DFT calculations.

In the middle of the last century, the discovery of the olefin polymerization reaction in the presence of transition metal salts or complexes by K. Ziegler and J. Natta led to a revolution in catalysis. The development of catalytic systems based on η^5-complexes of group 4B metals, and then post-metallocenes, in combination with Al- or B-containing activators, made it possible to transfer classical Ziegler catalysis from a heterogeneous to a homogeneous medium. As a result, highly efficient single-site homogeneous catalysts for di-, oligo-, and polymerization reactions of olefins and dienes were developed.[1–6] It is assumed that the activity, regio- and stereoselectivity in these reactions are controlled mainly by the π- or σ-ligand environment of the transition metal atom in the catalytically active sites. However, B- or Al-containing cocatalysts contribute to the organization of catalytically active sites as well. Their association with a transition metal salt or a complex provides an ion pair, which then dissociates, giving an active cationic site, or in which the anion is replaced by a monomer.[7] Experimental studies[8,9] and theoretical analysis[10] indicate the imperfection of the model which considers only the cationic center and the importance of taking into account the counter ion.

Thus, the development of modern models of Ziegler–Natta catalysis, taking into account the knowledge accumulated to date about the catalytically active center structure and principles of action, is an important and topical task. One of the most promising approaches to solving this problem is chiral recognition, which provides detailed information on the organization and behavior of the catalytic system. In this research, we have carried out quantum chemical modeling of the stages of alkene coordination using propene and hex-1-ene as the examples by chiral catalytically active centers obtained as a result of $Cp_2ZrMeCl$ coordination with the methylalumoxane (MAO) activator containing prochiral centers.

The PRIRODA-09 program developed by Laikov[11–13] was used to perform quantum chemical calculations. These calculations included various tasks such as geometric optimization of complexes, analysis of vibrational frequencies, search for transition states, scanning along the internal reaction coordinate, calculation of entropy and thermodynamic corrections to the total energy of compounds. Thermodynamic parameters were determined for standard conditions (298.15 K, 1 atm) in the gas phase. The DFT level was used for these calculations, and the Perdew–Burke–Ernzerhof (PBE)[14] functional was combined with a 3ζ basis set (see Online Supplementary Materials).[11,13] The triple split valence basis 3ζ, developed by Laikov is a nonrelativistic Gaussian-type atomic basis set containing a diffuse part and polarization functions. The electronic configurations of the molecular systems were described by the orbital basis sets of contracted Gaussian-type functions of size (5s2p)/[3s1p] for H, (11s6p2d)/[6s3p2d] for C and O, (15s11p2d)/[10s6p2d] for Al and Cl, and (20s16p11d)/[14s11p7d] for Zr, which were used in combination with the density-fitting basis sets of uncontracted Gaussian-type functions of size (5s2p) for H, (10s3p3d1f) for C and O, (14s3p3d1f1g) for Al and Cl, and (22s5p5d4f4g) for Zr. We choose PBE/3ζ method because it satisfactorily describes the energetic parameters of the reactions taking place in Zr,Al-systems as well as M06-2X, as previously shown.[15–18] Energetic parameters of all intermediates were also calculated using Gaussian 09 software[19] by the M06-2X functional[20] in combination with Dunnings correlation consistent cc-pVDZ basis set for H, C, O, Cl and Al,[21–23] and the relativistically corrected effective core potential containing cc-pVDZ-PP basis set for Zr[24] (as obtained from the EMSL Basis Set Exchange).[25] Visualization of quantum chemical data was carried out using the programs QCC Front-End[26] and ChemCraft.[27]

For quantum chemical study, we consider a complex generated in the course of the reaction of zirconocene methyl chloride with MAO model $Me_{11}Al_{11}O_{10}$, whose structure contains both cage and chain fragments [Figure 1(*a*)]. It was previously established that the complex is easily formed (ΔH = –23.7 kcal mol^{-1}).[28]

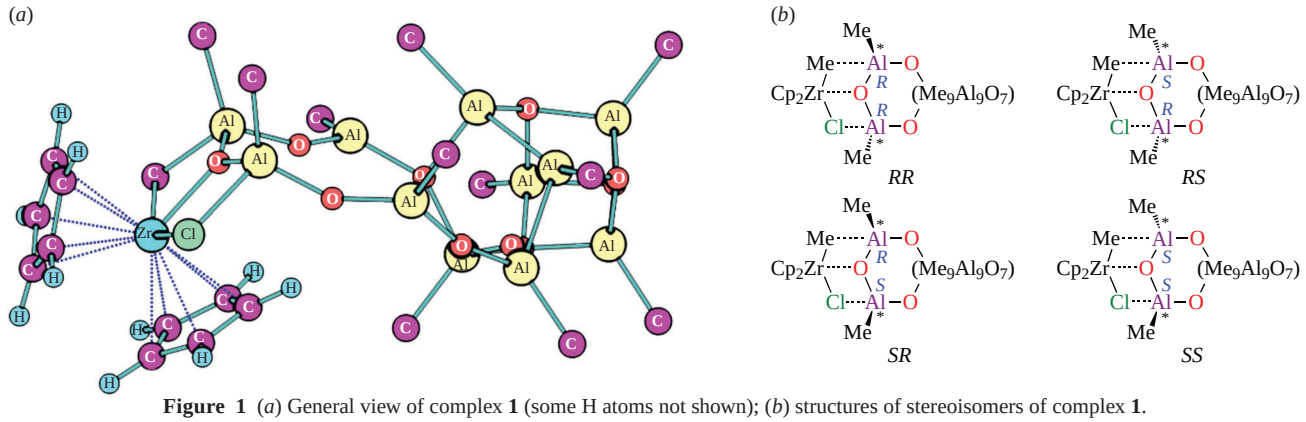

Figure 1 (*a*) General view of complex **1** (some H atoms not shown); (*b*) structures of stereoisomers of complex **1**.

Moreover, asymmetric centers appear on aluminum atoms in this complex; therefore, catalytically active complex $Cp_2ZrMeCl–Me_{11}Al_{11}O_{10}$ could exist as a set of possible stereoisomers [Figure 1(*b*)].

We evaluated stability of complex **1** stereoisomers by calculating the relative thermodynamic parameters under standard conditions (Table 1). The calculated data on the thermodynamic stability of stereoisomeric complexes of zirconocene methyl chloride with MAO differ slightly for PBE/3ζ and M06-2X methods. Thus, it turned out that the *S*,*S*-isomer is the most energetically favorable (according to the value of ΔH); however, when taking into account the entropy correction, the stereoisomer with the *R*,*R*-configuration of the chiral centers at the Al atoms is more stable at 298 K according to the PBE/3ζ method [see Figure 1(*b*)]. Therefore, one should expect the predominance of the *S*,*S*-stereomer (and/or *R*,*R*-stereomer) among the possible structures. The observed energy difference between, for example, the *R*,*R*- and *S*,*S*-stereoisomers is significant, and reaches 1.8 kcal mol^{-1} according to the data of the M06-2X/cc-pVDZ//cc-pVDZ-PP method, which is apparently due to the influence of the MAO fragment containing a conformationally flexible spacer and a cluster fragment (for details, see Online Supplementary Materials).

To reveal the influence of the active site stereochemistry on the energy parameters of the alkene carbometalation as the first step of oligomerization reaction, we simulated the interaction of complex **1** with both propene **2** and hex-1-ene **4** molecules (Scheme 1).

The orientation of the alkene molecules was modeled according to the described approach.[29] As follows from Table 2, the thermodynamic and activation parameters of reaction for both alkenes with four possible complex **1** stereoisomers differ significantly. Thus, both methods showed that, for example, for propene *si* insertion (reactions 1–4), the *R*,*R*-isomer of complex **1** is more reactive, whereas the *S*,*S*-stereoisomer should not react under standard conditions, while the maximum $\Delta\Delta G^{\neq}_{max}$ ($\Delta G^{\neq}_{RR} - \Delta G^{\neq}_{SS}$) reaches 20.6 kcal mol^{-1} (25.2 kcal mol^{-1} by M06-2X). Probably, the difference in values is due to the steric effects of Cp-ligands and Al–Me fragments of the reaction center.

Table 1 Relative values of thermodynamic parameters[a] of complex **1** stereoisomers under standard conditions.

Diastereomer	PBE/3ζ			M06-2X/cc-pVDZ//cc-pVDZ-PP		
	ΔH	ΔG	ΔS	ΔH	ΔG	ΔS
RR	1.2	0.0	9.1	1.4	1.8	2.8
RS	1.1	0.7	6.5	4.0	2.2	10.1
SR	0.8	2.3	0.1	2.7	3.9	0.0
SS	0.0	1.6	0.0	0.0	0.0	4.1

[a] [ΔS] = cal mol^{-1} K^{-1}; [ΔH] = [ΔG] = kcal mol^{-1}.

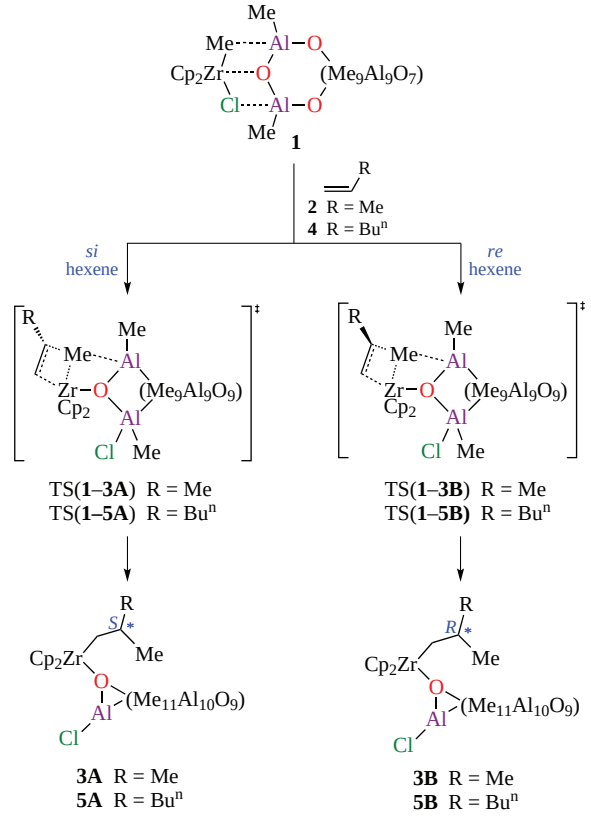

Scheme 1 1,2-Insertion of alkenes into the Zr–C bond of complex **1** with *si* and *re* orientations of the substrate.

Moreover, the process of alkene insertion into complex **1** is also thermodynamically favorable (see Table 2, entry 1). The energy gain is achieved due to the transfer of a chlorine atom from the Zr atom to the Al_{MAO} atom and rearrangement of the MAO fragments in the reaction products (Figure 2).

It should be noted that the formation of a structural pattern of the **3A_*SS*** type is less thermodynamically favorable and leads to a significant change in the reaction enthalpies, for example, $\Delta H_{RR} - \Delta H_{SS}$ = 25.1 kcal mol^{-1} (PBE). Conformational effects of the growing alkyl chain could also contribute to the energy difference.

Analysis of the obtained data for propene *re* insertion (see Table 2, entries 5–8) showed that the formation of the **3_*RR*** stereoisomer is characterized by an activation barrier, which is 1.9 (PBE) or 1.8 kcal mol^{-1} (for M06-2X) lower compared to entry 1, although the product **3B_*RR*** is less thermodynamically stable. It should be noted that for the *re* insertion of a propene molecule, there is no significant difference ($\Delta\Delta G^{\neq}$ = 0.4 for PBE and 0.9 kcal mol^{-1} for M06-2X) between the insertion barriers ($\Delta G^{\neq}_{SS} - \Delta G^{\neq}_{RR}$). In this series of calculations (entries 5–8), reaction of entry 7 has relatively greater kinetic and thermo-

Table 2 Thermodynamic parameters[a] of reactions[b] **1**→**3** and **1**→**5** under standard conditions.

Entry	Reaction	PBE/3ζ						M06-2X/cc-pVDZ//cc-pVDZ-PP					
		$\Delta H°$	$\Delta G°$	$\Delta S°$	$\Delta H^{\neq}$	$\Delta G^{\neq}$	$\Delta S^{\neq}$	$\Delta H°$	$\Delta G°$	$\Delta S°$	$\Delta H^{\neq}$	$\Delta G^{\neq}$	$\Delta S^{\neq}$
1	**1_*RR*** + **2** → **3A_*RR***	–28.4	–12.6	–53.1	22.7	38.9	–54.1	–39.8	–28.2	–38.9	15.7	28.4	–42.6
2	**1_*RS*** + **2** → **3A_*RS***	–18.2	0.9	–63.9	31.8	49.9	–60.8	–38.1	–22.0	–54.3	17.8	35.7	–60.1
3	**1_*SR*** + **2** → **3A_*SR***	–9.9	2.4	–41.1	41.4	55.4	–47.1	–17.7	–5.2	–41.9	40.6	56.8	–54.5
4	**1_*SS*** + **2** → **3A_*SS***	–3.3	9.4	–42.6	43.8	59.5	–52.5	–14.6	0.3	–50.0	41.0	53.6	–42.2
5	**1_*RR*** + **2** → **3B_*RR***	–14.2	1.0	–50.9	18.8	37.0	–61.0	–17.7	–7.3	–34.8	18.9	30.2	–38.1
6	**1_*RS*** + **2** → **3B_*RS***	–9.8	5.3	–50.6	42.2	57.4	–50.9	–18.1	–5.0	–44.1	42.3	57.2	–50.1
7	**1_*SR*** + **2** → **3B_*SR***	–31.6	–16.6	–50.4	20.0	35.4	–51.7	–46.5	–32.0	–48.4	12.3	24.8	–41.6
8	**1_*SS*** + **2** → **3B_*SS***	–27.8	–16.6	–37.6	23.7	37.4	–46.1	–38.7	–25.3	–45.0	15.9	31.1	–50.7
9	**1_*RR*** + **4** → **5A_*RR***	–23.0	–7.0	–53.9	23.7	41.1	–58.3	–37.3	–22.5	–49.8	16.2	27.6	–38.3
10	**1_*RS*** + **4** → **5A_*RS***	–17.6	1.1	–62.9	31.5	50.0	–62.0	–40.0	–22.0	–60.4	18.0	34.9	–56.5
11	**1_*SR*** + **4** → **5A_*SR***	–9.2	3.8	–43.6	41.0	54.9	–46.8	–17.8	–5.1	–42.5	41.5	54.1	–42.2
12	**1_*SS*** + **4** → **5A_*SS***	–2.7	10.2	–43.0	43.5	59.8	–54.7	–16.4	–0.3	–54.0	39.8	53.4	–45.6
13	**1_*RR*** + **4** → **5B_*RR***	–13.6	1.8	–51.6	18.8	36.2	–58.1	–18.4	–7.2	–37.4	17.9	30.8	–43.1
14	**1_*RS*** + **4** → **5B_*RS***	–9.1	5.7	–49.7	41.9	57.5	–52.0	–18.4	–5.2	–44.3	39.5	58.4	–63.3
15	**1_*SR*** + **4** → **5B_*SR***	–30.9	–15.7	–51.2	19.8	35.7	–53.5	–45.1	–32.6	–41.9	12.3	24.5	–41.0
16	**1_*SS*** + **4** → **5B_*SS***	–26.4	–12.8	–45.8	23.8	37.8	–47.1	–39.2	–24.6	–49.1	16.5	31.4	–49.8

[a] $[\Delta S]$ = cal mol^{-1} K^{-1}; $[\Delta H] = [\Delta G]$ = kcal mol^{-1}. [b] *R*,*S* designation is given for the MAO fragment in the reaction products.

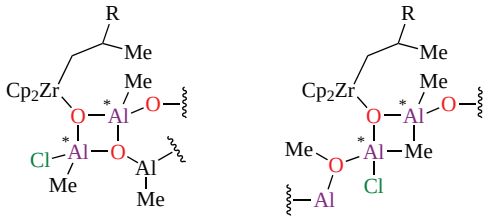

3A_*RR*, **3B_*SR***, **3B_*SS***, **5A_*RR***, **5B_*SR***, **5B_*SS***

3A_*RS*, **3A_*SR***, **3A_*SS***, **3B_*RS***, **5A_*RS***, **5A_*SR***, **5A_*SS***, **5B_*RS***

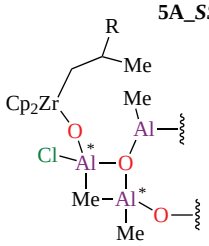

3B_*RR*, **5B_*RR***

Figure 2 Specific structural patterns characteristic to products **3** and **5**.

dynamic advantage. The reaction also provides a product with the *R*-configuration of chiral centers on Al atoms. If we compare the activation barriers of reactions 2 and 6, which give the same structural patterns of the products, the difference $\Delta\Delta G$(**3A**$_{RS}$ – **3B**$_{RS}$) = 7.5 (PBE) and 21.5 kcal mol^{-1} (M06-2X) clearly demonstrates the significant contribution of alkene *re* and *si* orientation in the course of coordination. The above tendencies of changes in the activation barriers of reactions 1–8 are generally also characteristic to reactions 9–16 for hex-1-ene insertion. The difference is that the formation barrier for **5A_*RR*** (*si* orientation) is greater than the one for **5B_*RR*** (*re* orientation) according to PBE data, while the opposite relation is observed in the case of using M06-2X; nevertheless, the difference $\Delta\Delta G^{\neq}$ remains significant and reaches ~3.2 kcal mol^{-1} (see Table 2).

To conclude, using the PBE/3ζ and M06-2X/cc-pVDZ//cc-pVDZ-PP methods, we calculated the relative thermodynamic stability of stereoisomeric complexes of zirconocene methyl chloride with MAO model $Me_{11}Al_{11}O_{10}$ (hybrid cage and chain model) and established the energy profit of isomers with *S*,*S*- and *R*,*R*-configurations of chiral centers on Al atoms of the catalytically active center. It is shown that the value of the barrier of alkene insertion into catalytically active sites (*re* and *si* coordination) largely depends on the relative configuration of chiral centers in the activator, which indicates its potential contribution to stereoregulation at the stage of substrate coordination in the course of the oligomerization reaction. The results obtained also indicate a possible contribution of the linear MAO structure to the activation of metal complexes, while the cluster structures are usually considered responsible for the formation of cationic species acting as highly active polymerization sites.[30–32] However, it was reported[33] that in addition to the 'classical' structure MAO, in which highly reactive Al–O bonds inside 3D frameworks act as reaction centers, there is another active or 'true' MAO structure, in which the reaction centers are represented by three-coordinated aluminum atoms in =O–AlMe$_2$ groups. These groups are formed in the 'true' MAO when the AlMe$_3$ molecule is attached to the 'classical' activator molecule. In our model, we have shown that linear –O–Al(Me)–O–Al(Me)–O– fragments can act as activating groups, significantly reducing the barrier of alkene insertion into the Zr–C bond and providing thermodynamically favorable conditions for the process due to the elimination of the chlorine atom from the zirconium center and the rearrangement of the MAO structure as part of the active intermediate.

This work was financially supported by Russian Science Foundation (grant no. 22-73-00280).

Online Supplementary Materials

Supplementary data associated with this article can be found in the online version at doi: 10.1016/j.mencom.2023.09.022.

References

1 C. Janiak, *Coord. Chem. Rev.*, 2006, **250**, 66.
2 R. L. Shubkin and M. E. Kerkemeyer, *J. Synth. Lubr.*, 1991, **8**, 115.
3 S. Ray, P. V. C. Rao and N. V. Choudary, *Lubr. Sci.*, 2012, **24**, 23.
4 K. S. Whiteley, T. G. Heggs, H. Koch, R. L. Mawer and W. Immel, in *Ullmann's Encyclopedia of Industrial Chemistry*, Wiley, Weinheim, 2000.
5 I. Nifant'ev, P. Ivchenko, A. Tavtorkin, A. Vinogradov and A. Vinogradov, *Pure Appl. Chem.*, 2017, **89**, 1017.
6 I. Nifant'ev and P. Ivchenko, *Polymers*, 2020, **12**, 1082.
7 M. Bochmann, *J. Organomet. Chem.*, 2004, **689**, 3982.
8 A. Xiao, L. Wang, Q. Liu and X. Dong, *Des. Monomers Polym.*, 2007, **10**, 281.

9 L. V. Parfenova, P. V. Kovyazin, A. K. Bikmeeva, E. R. Palatov, P. V. Ivchenko, I. E. Nifant'ev and L. M. Khalilov, *Molecules*, 2023, **28**, 2420.
10 K. Matsumoto, M. Takayanagi, S. K. Sankaran, N. Koga and M. Nagaoka, *Organometallics*, 2018, **37**, 343.
11 D. N. Laikov, *PhD Thesis*, M. V. Lomonosov Moscow State University, 2000 (in Russian).
12 D. N. Laikov and Yu. A. Ustynyuk, *Russ. Chem. Bull.*, 2005, **54**, 820 (*Izv. Akad. Nauk, Ser. Khim.*, 2005, 804).
13 D. N. Laikov, *Chem. Phys. Lett.*, 1997, **281**, 151.
14 J. P. Perdew, K. Burke and M. Ernzerhof, *Phys. Rev. Lett.*, 1996, **77**, 3865.
15 E. Yu. Pankratyev, T. V. Tyumkina, L. V. Parfenova, S. L. Khursan, L. M. Khalilov and U. M. Dzhemilev, *Organometallics*, 2011, **30**, 6078.
16 T. V. Tyumkina, D. N. Islamov, L. V. Parfenova, R. J. Whitby, L. M. Khalilov and U. M. Dzhemilev, *J. Organomet. Chem.*, 2016, **822**, 135.
17 Y. Sun and H. Chen, *J. Chem. Theory Comput.*, 2013, **9**, 4735.
18 I. E. Nifant'ev, L. Yu. Ustynyuk and D. N. Laikov, *Organometallics*, 2001, **20**, 5375.
19 M. J. Frisch, G. W. Trucks, H. B. Schlegel, G. E. Scuseria, M. A. Robb, J. R. Cheeseman, G. Scalmani, V. Barone, B. Mennucci, G. A. Petersson, H. Nakatsuji, M. Caricato, X. Li, H. P. Hratchian, A. F. Izmaylov, J. Bloino, G. Zheng, J. L. Sonnenberg, M. Hada, M. Ehara, K. Toyota, R. Fukuda, J. Hasegawa, M. Ishida, T. Nakajima, Y. Honda, O. Kitao, H. Nakai, T. Vreven, J. A. Montgomery, Jr., J. E. Peralta, F. Ogliaro, M. Bearpark, J. J. Heyd, E. Brothers, K. N. Kudin, V. N. Staroverov, T. Keith, R. Kobayashi, J. Normand, K. Raghavachari, A. Rendell, J. C. Burant, S. S. Iyengar, J. Tomasi, M. Cossi, N. Rega, J. M. Millam, M. Klene, J. E. Knox, J. B. Cross, V. Bakken, C. Adamo, J. Jaramillo, R. Gomperts, R. E. Stratmann, O. Yazyev, A. J. Austin, R. Cammi, C. Pomelli, J. W. Ochterski, R. L. Martin, K. Morokuma, V. G. Zakrzewski, G. A. Voth, P. Salvador, J. J. Dannenberg, S. Dapprich, A. D. Daniels, O. Farkas, J. B. Foresman, J. V. Ortiz, J. Cioslowski and D. J. Fox, *Gaussian 09, Revision D.01*, Gaussian, Wallingford, CT, 2013.
20 Y. Zhao and D. G. Truhlar, *Theor. Chem. Acc.*, 2007, **120**, 215.
21 T. H. Dunning, *J. Chem. Phys.*, 1989, **90**, 1007.
22 D. E. Woon and T. H. Dunning, Jr., *J. Chem. Phys.*, 1993, **98**, 1358.
23 E. R. Davidson, *Chem. Phys. Lett.*, 1996, **260**, 514.
24 K. A. Peterson, D. Figgen, M. Dolg and H. Stoll, *J. Chem. Phys.*, 2007, **126**, 124101.
25 K. L. Schuchardt, B. T. Didier, T. Elsethagen, L. Sun, V. Gurumoorthi, J. Chase, J. Li and T. L. Windus, *J. Chem. Inf. Model.*, 2007, **47**, 1045.
26 D. V. Besedin, *Quantum Chemistry Calculations (QCC) Front-End 2.09*, 2005.
27 G. A. Zhurko and D. A. Zhurko, *ChemCraft 1.6*, 2009.
28 T. V. Tyumkina, D. N. Islamov, P. V. Kovyazin and L. V. Parfenova, *Mol. Catal.*, 2021, **512**, 111768.
29 C. De Rosa, R. Di Girolamo, A. B. Muñoz-García, M. Pavone and G. Talarico, *Macromolecules*, 2020, **53**, 2959.
30 E. Zurek and T. Ziegler, *Prog. Polym. Sci.*, 2004, **29**, 107.
31 F. Zaccaria, P. H. M. Budzelaar, R. Cipullo, C. Zuccaccia, A. Macchioni, V. Busico and C. Ehm, *Inorg. Chem.*, 2020, **59**, 5751.
32 V. E. Teixeira and P. R. Livotto, *J. Mol. Graph. Model.*, 2020, **99**, 107626.
33 V. A. Zakharov, I. I. Zakharov and V. N. Panchenko, in *Organometallic Catalysts and Olefin Polymerization*, eds. R. Blom, A. Follestad, E. Rytter, M. Tilset and M. Ystenes, Springer, Berlin, Heidelberg, 2001, pp. 63–71.

Received: 24th March 2023; Com. 23/7130